Molecular Neurobiology (2019) 56:7863–7871
https://doi.org/10.1007/s12035-019-01648-z

ORIGINAL PAPER

Rheologically Essential Surfactant Proteins of the CSF Interacting with Periventricular White Matter Changes in Hydrocephalus Patients – Implications for CSF Dynamics and the Glymphatic System

Alexander Weiß[1] · Matthias Krause[2] · Anika Stockert[3] · Cindy Richter[1] · Joana Puchta[1,4] · Pervinder Bhogal[5] · Karl-Titus Hoffmann[1] · Alexander Emmer[6] · Ulf Quäschling[1] · Cordula Scherlach[1] · Wolfgang Härtig[4] · Stefan Schob[1]

Received: 25 February 2019 / Accepted: 13 May 2019 / Published online: 24 May 2019

Abstract

Surfactant proteins (SP) are multi-systemic proteins playing crucial roles in the regulation of rheological properties of physiological fluids, host defense, and the clearance of potentially harmful metabolites. Hydrocephalus patients suffer from disturbed central nervous system (CNS) fluid homeostasis and exhibit remarkably altered SP concentrations within the cerebrospinal fluid (CSF). A connection between CSF-SPs, CSF flow, and ventricular dilatation, a morphological hallmark of hydrocephalus, has been reported previously. However, currently there are no studies investigating the link between rheologically active SPs and periventricular white matter changes caused by impaired CSF microcirculation in hydrocephalic conditions. Thus, the aim of this study was to assess their possible relationships. The present study included 47 individuals (27 healthy subjects and 20 hydrocephalus patients). CSF specimens were analyzed for concentrations of SP-A, SP-C, and SP-D by using enzyme-linked immunosorbent assays (ELISAs). Axial T2w turbo inversion recovery magnitude (TIRM) magnetic resonance imaging was employed in all cases. Using a custom-made MATLAB-based tool for quantification of magnetic resonance signal intensities in the brain, parameters related to disturbed deep white matter CSF microcirculation were estimated (TIRM signal intensity (SI)—mean, minimum, maximum, median, mode, standard deviation, and percentiles, p10th, p25th, p75th, p90th, as well as kurtosis, skewness, and entropy of the SI distribution). Subsequently, statistical analysis was performed (IBM SPSS 24™) to identify differences between hydrocephalic patients and healthy individuals and to further investigate the connections between CSF-SP changes and deep white matter signal intensities. SP-A (0.38 ± 0.23 vs. 0.76 ± 0.49 ng/ml) and SP-C (0.54 ± 0.28 vs. 1.27 ± 1.09 ng/ml) differed between healthy controls and hydrocephalus patients in a statistically significant manner. Also, corresponding quantification of white matter signal intensities revealed statistically significant differences between hydrocephalus patients and healthy individuals: SImean (370.41 ± 188.15 vs. 222.27 ± 99.86, $p = 0.001$), SImax (1115.30 ± 700.12 vs. 617.00 ± 459.34, $p = 0.005$), SImedian (321.40 ± 153.17 vs. 209.52 ± 84.86, $p = 0.001$), SImode (276.55 ± 125.63 vs. 197.26 ± 78.51, $p = 0.011$), SIstd (157.09 ± 110.07 vs. 81.71 ± 64.94, $p = 0.005$), SIp10 (229.10 ± 104.22 vs. 140.00 ± 63.12, $p = 0.001$), SIp25 (266.95 ± 122.62 vs. 175.63 ± 71.42, $p = 0.002$), SIp75 (428.80 ± 226.88 vs. 252.19 ± 110.91, $p = 0.001$), SIp90 (596.47 ± 345.61 vs. 322.06 ± 176.00, $p = 0.001$), skewness (1.19 ± 0.68 vs. 0.43 ± 1.19, $p = 0.014$), and entropy (5.36 ± 0.37 vs. 4.92 ± 0.51, $p = 0.002$). There were no differences regarding SP-D levels in hydrocephalus patients vs. healthy controls. In the acute hydrocephalic subgroup, correlations were as follows: SP-A showed a statistically significant correlation with SImax ($r = 0.670$, $p =$

Alexander Weiß, Matthias Krause, Wolfgang Härtig and Stefan Schob contributed equally to this work.

✉ Stefan Schob
stefan.schob@medizin.uni-leipzig.de

[1] Department of Neuroradiology, University Hospital Leipzig, Liebigstrasse 20, 04103 Leipzig, Germany

[2] Department of Neurosurgery, University Hospital Leipzig, Leipzig, Germany

[3] Department of Neurology, University Hospital Leipzig, Leipzig, Germany

[4] Paul Flechsig Institute for Brain Research, University Leipzig, Leipzig, Germany

[5] Department of Interventional Neuroradiology, Royal London Hospital, London, UK

[6] Department for Neurology, University Hospital Halle-Wittenberg, Halle, Germany

0.024), SIstd ($r = 0.697$, $p = 0.017$), SIp90 ($r = 0.621$, $p = 0.041$), and inverse correlation with entropy ($r = -0.700$, $p = 0.016$). SP-C correlated inversely with entropy ($r = -0.686$, $p = 0.020$). For the chronic hydrocephalus subgroup, the following correlations were identified: SP-A correlated with kurtosis of the TIRM histogram ($r = -0.746$, $p = 0.021$). SP-C correlated with SImean ($r = -0.688$, $p = 0.041$), SImax ($r = -0.741$, $p = 0.022$), SImedian ($r = -0.716$, $p = 0.030$), SImode ($r = -0.765$, $p = 0.016$), SIstd ($r = -0.671$, $p = 0.048$), SIp25 ($r = -0.740$, $p = 0.023$), SIp75 ($r = -0.672$, $p = 0.048$), and SIp90 ($r = -0.667$, $p = 0.050$). SP-D apparently does not play a major role in CSF fluid physiology. SP-A and SP-C are involved in different aspects of CNS fluid physiology. SP-A appears to play an essential compensatory role in acute hydrocephalus and seems less involved in chronic hydrocephalus. In contrary, SP-C profile and white matter changes are remarkably connected in CSF of chronic hydrocephalus patients. Considering the association between CSF flow phenomena, white matter changes, and SP-C profiles, the latter may especially contribute to the regulation of paravascular glymphatic physiology.

Keywords MRI · Histogram analysis · Surfactant proteins · CSF · TIRM · Glymphatic

Introduction

Molecules within a fluid are exposed to attractive forces by all the surrounding molecules. In a homogeneous fluid continuum, the sum of the resulting forces is zero and no intermolecular force related–tension is generated. Contrarily, the surface of a fluid that borders a physico-chemically distinct compartment—as exemplarily the air-water interface—naturally exhibits substantial surface tension. This is mostly the result of inherently formed hydrogen bonds between dipolar water molecules, which cannot evenly be formed at the air-water interface. As a consequence, a highly attractive net force results, which pulls molecules towards the inside of the fluid and causes its surface to contract and bead up [1]. This phenomenon naturally also occurs in physiological fluids like tear fluid and cerebrospinal fluid (CSF), although its impact is considered most significant for the alveolar fluid [2, 3]. Accordingly, the tight regulation of surface tension and viscosity is of crucial importance for proper physiology, most importantly for respiratory function [4].

Surface tension and its pathologic alterations accompanying distinct diseases were studied extensively in the lungs. Here, the pulmonary surface active agent (surfactant), a complex lipo-protein mixture which covers the alveolar fluid layer, accomplishes the physiologically essential reduction of alveolar surface tension and hereby only then renders respiratory mechanics possible. However, abundance of amphiphilic surfactant proteins (SPs) A, B, C, and D is essential for surfactant functionality [5, 6].

Surfactant deficiency, as exemplarily present in prematurely newborn infants, causes the commonly fatal hyaline membrane syndrome [7, 8]. Thereby, lack of surfactant results in insuperable intra-alveolar surface tension, which leads to a detrimental cascade that eventually culminates in alveolar collapse and finally, death by pulmonary failure [9].

SP deficiency can successfully be treated by intratracheal administration of SP-containing preparations, which drastically reduce the mortality [10, 11].

Nowadays, SPs are being increasingly recognized as important, multifunctional molecular players of extra-pulmonary physiology, exemplarily in the central nervous system (CNS) [12, 13]. More specifically, antibody-equivalent, collectin-types SP-A and SP-D are involved in CNS innate immunity and clearance of cellular waste and CSF homeostasis [14–19]. Their much smaller, more hydrophobic companions SP-B and SP-C were reported to be primarily involved in the regulation of CSF rheology. SP-C—among the most surface active proteins known—exhibits significant alterations in conditions with a disturbed CSF flow, while SP-B remains at roughly the same concentration in diseases related to impaired CSF circulation [15]. However, SP-C is not associated with the CSF bulk flow in cranial magnetic resonance imaging [16]. Considering previous reports on SP expression pattern in the CNS and the distinct regulation of each SP in different conditions related to altered CSF flow, these findings allude to SPs' importance for microcirculatory CSF dynamics along the perivascular route [20–22].

So far, the relationship of rheologically active SPs in the CSF and periventricular white matter changes caused by impaired CSF microcirculation [23] in hydrocephalus patients has not yet been investigated. Therefore, our study is aimed at (a) quantitatively determining periventricular white matter changes in hydrocephalus patients using a histogram-based approach on fluid-sensitive magnetic resonance images, (b) quantifying rheologically important SPs in corresponding CSF samples, and (c) determining the extent of their connection using correlative statistics.

Materials and Methods

Ethics Approval

This retrospective study was approved by an institutional review board (Ethikkommission Universität Leipzig Az 330-13-18 112 013).

Patients

In total, 47 patients (24 females and 23 males) were included in our analysis. Informed consent for the scientific use of CSF samples, clinical, and radiological data was given in writing from all patients or caregivers. As a first step, the patients and CSF samples were checked for CNS infections and other inflammatory or autoimmune conditions. In such cases, the patients were excluded from the study. Furthermore, none of the cases exhibited significant leakage of serum proteins into the CSF. Twenty-seven patients without any proof of a neurological pathology served as the control group. These 27 CSF specimens were obtained within the standardized diagnostic algorithm of our center including lumbar puncture for exclusion of subarachnoid hemorrhage (SAH), meningitis, or demyelinating disease. A total of 20 CSF samples of patients with clinically and neuroradiologically proven communicating hydrocephalus were included. Depending on the pathophysiology, they were classified as follows: aqueductal stenosis (AQS), acute hydrocephalus (AH) without AQS, and normal pressure hydrocephalus (NPH). Five patients with narrowed mesencephalic aqueduct and consecutively dilated lateral and third ventricles were categorized as AQS [15, 17]. The group of AH consisted of six patients with acute hydrocephalus as a consequence of previously suffered SAH or purulent meningitis. All patients with AH showed signs of elevated intracranial pressure [24]. The majority of patients (9) was categorized under the NPH group and met the following neuroimaging (ventriculomegaly and narrow convexity of the sulcus in combination with dilated Sylvian fissures) and clinical criteria (dementia, incontinence, gait ataxia).

Table 1 gives an overview of the demographic distribution of hydrocephalus and control patients. Additionally, Table 2 characterizes the demographic properties of the hydrocephalus subgroups.

Determination of Surfactant Protein Concentrations in CSF

SP concentrations were quantified using enzyme-linked immunosorbent assays (ELISAs) according to the manufacturer's manual. Commercially available ELISA kits (USCN, Wuhan, China) were used for quantification of SP-A (E90890Hu, ELISA kit for surfactant-associated protein A), SP-C (E91623Hu, ELISA kit for surfactant-associated protein C), and SP-D (E91039Hu, ELISA kit for surfactant-associated protein D) in the CSF samples. The analysis was performed using a microplate spectrophotometer (ELISA-reader) at a wavelength of 450 nm and a reference wavelength of 405 nm for absorbance measuring. Surfactant protein concentrations in nanograms per milliliter of CSF were calculated by comparison between standard series and the determined values of concentration according to the manufacturer's manual.

Table 1 Demographic data of healthy subjects and hydrocephalus patients

	Control group	Hydrocephalus patients
n	27	20
Age in years (mean, range)	43.8 2–78	44.8 < 1–84
Sex (female/male)	16/11	8/12

Magnetic Resonance Imaging

Cranial magnetic resonance imaging was performed in all patients using a 3-T device (Trio Tim, Siemens, /Germany). The imaging protocols differed between the investigated individuals depending on the initially suspected diagnosis. All imaging protocols necessarily included a fluid-sensitive sequence which is regularly used to assess changes of interstitial fluid (ISF) homeostasis—the fluid-attenuated inversion recovery (TIRM) sequence. This MRI technique is suitable for the quantification of white matter hyperintensities and reflects the extent of interstitial water content, secondary to impaired CSF flow [25–27].

Histogram Analysis of MR Imaging

As white matter hyperintensities have been studied using a variety of non-sufficiently comparable, rather subjective visual scoring systems, we used the volumetric histogram analysis technique which has been validated in numerous previous studies with structural correlations [28–31].

For this purpose, MR images were transferred in a DICOM format and processed offline with a custom-made MATLAB-programmed tool (The MathWorks, Natick, MA, USA) on a Windows-operated console. This tool displays MR images within a graphical user interface (GUI) and allows the analyst to scroll through the images. Regions of interest (ROIs) can then be drawn along the subject of interest which in our case was the periventricular white matter surrounding the lateral ventricles. The volumes of interest (VOI) was created by manually drawing ROIs along the lateral ventricles in every slice that showed a portion of the ventricles and adjacent periventricular white matter. The tool included the periventricular area of every slice with a diameter of 1 cm in every case. Every ROI was automatically modified in the GUI and saved (in a MATLAB-specific format) for later processing. All measures were performed by one author (UQ). After setting the VOIs, the following parameters were calculated and given in a spreadsheet format: first-order characteristics are mean (SImean), minimum (SImin), maximum (SImax),

Table 2 Demographic data of the investigated hydrocephalus subgroups (*AQS* aqueductal stenosis, *AH* acute hydrocephalus without AQS, *NPH* normal pressure hydrocephalus)

	Acute hydrocephalus		Chronic hydrocephalus
	AQS	AH	NPH
n	5	6	9
Age in years (mean, range)	43.6	13.7	66.2
	8–65	< 1–36	31–84
Sex (female/male)	2/3	4/2	2/7

median (SImedian), mode (SImode), standard deviation (SIstd), and the percentiles: 10th (SIp10), 25th (SIp25), 75th (SIp75), and 90th (SIp90) of SI values. Furthermore, histogram-based characteristics of the ROI (second-order)—kurtosis, skewness, and entropy—were estimated. All calculations were performed using in-build MATLAB functions. Figure 1 provides four exemplary cases of hydrocephalus (MRI sections and the corresponding SI histograms) with increasing deep white matter signal changes due to increased fluid content.

Statistical Analysis

The statistical analysis was performed using IBM SPSS 24™ (SPSS Inc., Chicago, IL, USA). At first, collected data was evaluated by means of descriptive statistics (mean, standard deviation, range, or frequencies). Additionally, comparison of CSF-SP concentrations and quantitatively estimated white matter abnormalities between hydrocephalus patients and controls were performed by means of ANOVA. P values < 0.05 were taken to indicate statistical significance in all instances. Normal distribution of data was evaluated and proven by using the Shapiro-Wilk test. Pearson's correlation coefficient was then performed to analyze the associations between CSF-SP concentrations and quantitative estimations of white matter hyperintensities.

Results

Histogram Evaluation of Periventricular White Matter and CSF-SP Concentrations in the Overall Collective

For reasons of clarity and comprehensibility, results of both—histogram-based analysis of periventricular white matter TIRM signal intensities in MRI and CSF-SP ELISAs—are presented in a spreadsheet format.

First and second order histogram characteristics of white matter TIRM signal intensities in the overall collective are presented in Table 3. Table 4 provides corresponding SP concentrations in the CSF.

Tables 5 and 6 compare results of histogram analysis reflecting white matter signal intensity levels and corresponding CSF-SP concentrations in the control group and hydrocephalus patients. In brief, all first- and second-order parameters except for the minimum of signal intensity and kurtosis of the signal intensity distribution showed statistically significant differences between healthy subjects and hydrocephalus

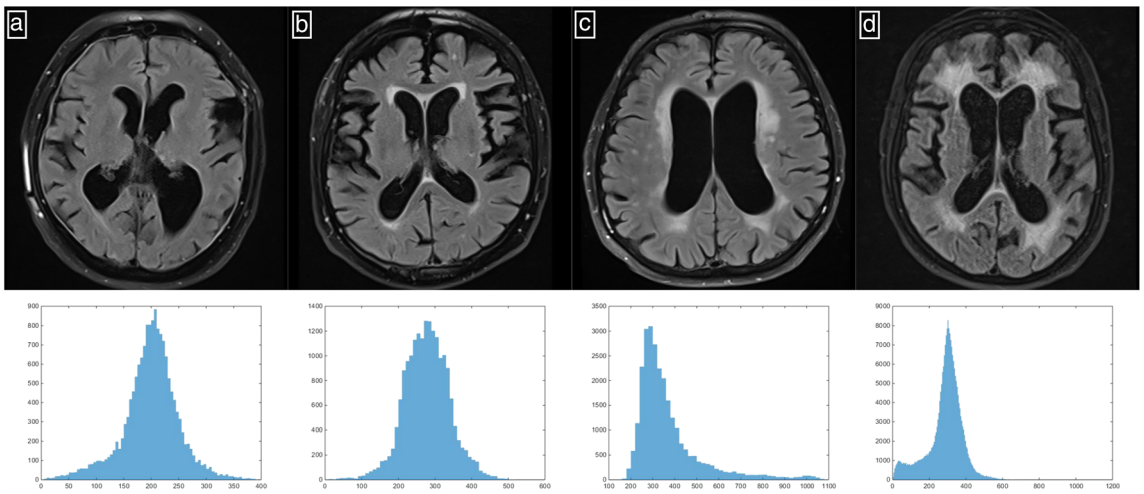

Fig. 1 Four exemplary hydrocephalus patients **a**–**d** exhibiting different extents of deep white matter fluid accumulation and the corresponding histograms

Table 3 White matter properties quantitatively evaluated by means of histogram analysis performed on TIRM-weighted MR images

	Overall collective	
	Mean ± SD	Range
SImean	285.31 ± 160.44	69.18–781.93
SImin	11.74 ± 21.83	1.00–109.00
SImax	829.04 ± 619.47	145.00–2522.00
SImedian	257.13 ± 129.95	71.00–638.00
SImode	231.00 ± 107.58	69.00–535.00
SIstd	113.79 ± 93.84	18.15–381.28
SIp10	177.92 ± 93.39	46.0–431.0
SIp25	214.49 ± 105.72	62.00–519.00
SIp75	327.34 ± 189.75	80.00–983.00
SIp90	438.83 ± 292.66	89.00–1364.00
Kurtosis	5.09 ± 1.71	2.94–11.56
Skewness	0.75 ± 1.07	−1.00 – 2.67
Entropy	5.10 ± 0.50	3.60–6.14

patients. Furthermore, SP-A and SP-C concentrations exhibited statistically significant differences between both groups, while SP-D did not display significantly different CSF-SP profiles. Figure 2 exemplarily provides corresponding boxplots comparing hydrocephalus patients with healthy subjects.

Correlation of White Matter Signal Alterations and SP Concentrations in the CSF

Finally, CSF-SP concentrations and signal intensity characteristics of periventricular white matter were correlated using Pearson's correlation coefficient, as Gaussian distribution was indicated by the Shapiro-Wilk test.

In the overall collective, no significant correlations between white matter characteristics and SP concentrations in CSF were found.

However, after analyzing the hydrocephalus patients as subgroup and further dividing them into an acute versus chronic stage hydrocephalus [15], the following results were observed.

Table 4 ELISA-derived CSF-SP concentrations (mean ± standard deviation) of all subjects are summarized here

	Overall collective	
	Mean ± SD	Range
SP-A (ng/ml)	0.54 ± 0.41	0.05–1.96
SP-C (ng/ml)	0.85 ± 0.82	0.12–5.18
SP-D (ng/ml)	6.61 ± 4.32	0.00–27.28

In the acute hydrocephalic subgroup, correlations were as follows: SP-A showed a statistically significant correlation with SImax ($r = 0.670$, $p = 0.024$), SIstd ($r = 0.697$, $p = 0.017$), SIp90 ($r = 0.621$, $p = 0.041$), and inverse correlation with entropy ($r = -0.700$, $p = 0.016$). SP-C correlated inversely with entropy ($r = -0.686$, $p = 0.020$).

For the chronic hydrocephalus subgroup, the following correlations were identified: SP-A correlated with kurtosis of the TIRM histogram ($r = -0.746$, $p = 0.021$). SP-C correlated with SImean ($r = -0.688$, $p = 0.041$), SImax ($r = -0.741$, $p = 0.022$), SImedian ($r = -0.716$, $p = 0.030$), SImode ($r = -0.765$, $p = 0.016$), SIstd ($r = -0.671$, $p = 0.048$), SIp25 ($r = -0.740$, $p = 0.023$), SIp75 ($r = -0.672$, $p = 0.048$) and SIp90 ($r = -0.667$, $p = 0.050$). Figure 3 exemplarily demonstrates correlations between CSF-SPs and findings of white matter signal analysis.

Discussion

This is the first study investigating the relationships between periventricular white matter signal intensities in fluid-sensitive MRI and corresponding CSF-SP profiles in the context of altered CSF circulation.

In accordance with earlier works, our current study confirmed that the amount of rheologically important SP-A and SP-C in samples of CSF from hydrocephalic patients differs considerably from those of healthy subjects [14–17].

As novel finding, corresponding periventricular white matter signal intensities—indicating different degrees of interstitial water content—also revealed differences of statistical significance when comparing healthy controls with hydrocephalus patients. More specifically, first-order and second-order characteristics of the periventricular white matter varied statistically significant between both groups, substantiating increased levels of ISF in the hydrocephalus group.

These findings are in line with recently published studies, which provided evidence for reduced periventricular clearance of ISF accompanied by ventricular reflux and transependymal congestion of CSF towards the deep white matter in hydrocephalus patients [32, 33].

This pathological decrease of ISF clearance along the glymphatic pathway is presumably of multifactorial nature with a structural- or functional aquaporin-4 deficiency in astrocytic perivascular end feet being one of its most essential pathomechanisms [24].

However, considering the remarkable glymphatic-like presence of SPs within the brain's perivascular spaces [13], their distinctly altered CSF pattern in conditions caused or accompanied by disturbed CSF homeostasis [14, 15, 17] and their correlation with apparent CSF flow phenomena in MRI [16], the cerebral SPs certainly contribute significantly in the regulation of glymphatic outflow and brain waste clearance.

Table 5 Comparison of quantified white matter changes in controls and hydrocephalus patients, also giving corresponding *p* values of ANOVA. Values given in italics indicate statistical significance

	Histogram parameters from controls ($n = 27$)		Histogram parameters from hydrocephalus patients ($n = 20$)		ANOVA
	Mean	SD	Mean	SD	*p*
SImean	222.27	99.86	370.41	188.15	*0.001*
SImin	11.56	20.41	12.00	24.16	0.946
SImax	617.00	459.34	1115.30	700.12	*0.005*
SImedian	209.52	84.86	321.40	153.17	*0.001*
SImode	197.26	78.51	276.55	125.63	*0.011*
SIstd	81.71	64.94	157.09	110.07	*0.005*
SIp10	140.00	63.12	229.10	104.22	*0.001*
SIp25	175.63	71.42	266.95	122.62	*0.002*
SIp75	252.19	110.91	428.80	226.88	*0.001*
SIp90	322.06	176.00	596.47	345.61	*0.001*
Kurtosis	5.30	1.93	4.81	1.35	0.343
Skewness	0.43	1.19	1.19	0.68	*0.014*
Entropy	4.92	0.51	5.36	0.37	*0.002*

This hypothesis is substantiated by their well-studied similar functions in other organs, for example at the air-tissue interface [34, 35]. Here, SPs serve two distinct purposes—host defense in the form of pathogen recognition receptor proteins and regulation of respiratory-wise essential physicochemical conditions via alteration of fluidity and surface tension of the alveolar fluid [34, 36].

More specifically, SP-A is probably of equal importance for CSF physiology as it enables proper respiratory function. Firstly, it maintains rheological properties of both fluids by scavenging pathologically leaked plasma proteins, which is a common feature of critical conditions in the respiratory tract and the CNS [14, 34, 37]. Secondly, it enhances the reduction of surface tension in both fluids directly and binds potentially harmful, local metabolic products in order to dispose of them, thereby essentially participating in the waste clearance of the lungs and brain. This is especially corroborated by earlier works that demonstrated the compensatory regulation of CSF-SP-A in conditions with altered CSF flow dynamics and the remarkable correlation of SP-A with CSF bulk flow in MRI [16]. Thirdly, it alleviates detrimental immune responses and acts as preformed antibody-equivalent, protecting vulnerable and exposed organ systems [19, 37]. The results of the present study indicate SP-A's participation predominantly in acute hydrocephalic states, as SP-A levels correlated significantly with signal intensities of periventricular white matter in this specific subgroup. Moreover, the kurtosis of distribution of white matter intensities in chronic hydrocephalus patients also correlated significantly with SP-A levels, suggesting SP-A's subsequent participation in the structural reorganization of the periventricular drainage in chronic hydrocephalus.

Interestingly, SP-C did not reveal any association with bulk flow in MRI of healthy subjects or patients suffering from conditions with disturbed CSF homeostasis [16]. However, our current study identified remarkable correlations between SP-C levels and periventricular white matter signal intensities in chronic hydrocephalus patients as well as an inverse correlation with the entropy of signal intensities in acute hydrocephalic conditions. These findings strongly suggest a specific SP-C contribution to microcirculatory CSF and ISF flow along the perivascular spaces within the deep white matter. In this context, it is of great importance to also reconsider another, well-reported aspect of SP-C functionality: SP-C is not only one of the most surface active proteins known; it also contains the so-called BRICHOS domain. This domain has

Table 6 Comparison of CSF-SP concentrations between controls and hydrocephalus patients, also displaying corresponding *p* values of ANOVA. Values given in italics indicate statistical significance

	CSF-SP levels, controls		CSF-SP levels, hydrocephalus patients		ANOVA
	Mean	SD	Mean	SD	*p*
SP-A (ng/ml)	0.38	0.23	0.76	0.49	*0.001*
SP-C (ng/ml)	0.54	0.28	1.27	1.09	*0.002*
SP-D (ng/ml)	6.01	2.09	7.41	6.16	0.278

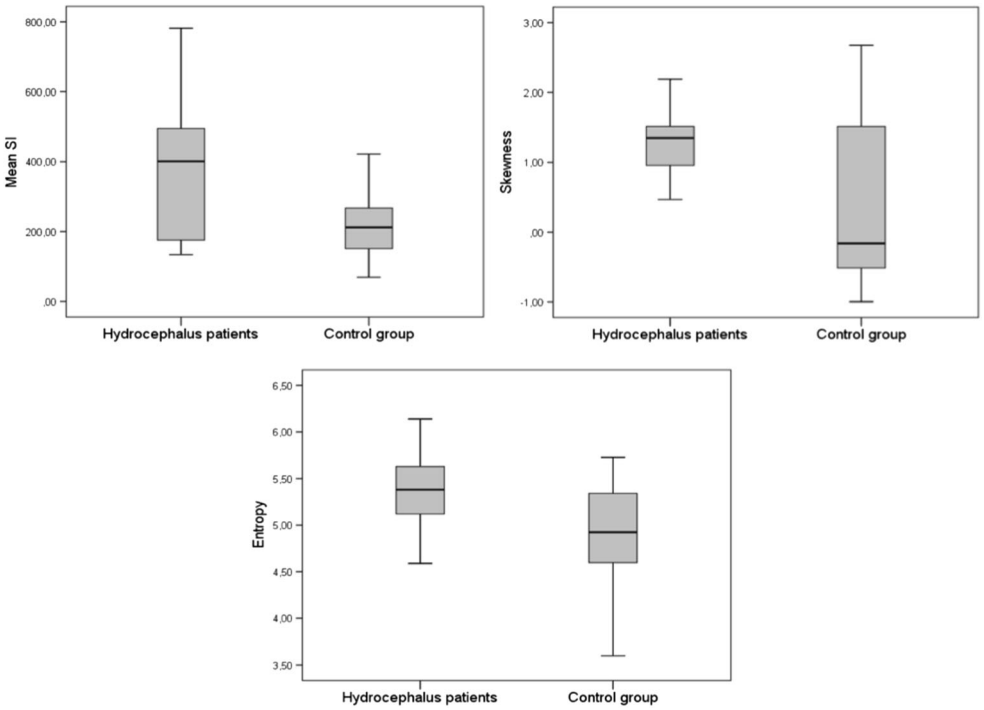

Fig. 2 Exemplary boxplots comparing first- and second-order characteristics of normal subjects and hydrocephalus patients. Statistically significant differences for all first- and second-order histogram characteristics were identified, except for SImin as well as for kurtosis. The findings indicate differences in white matter fluid content and distribution comparing both groups

been demonstrated to counteract protein misfolding in various organs [38]. Conversely, mutations affecting the BRICHOS domain have been postulated to be responsible for amyloid-related conditions like interstitial lung diseases and type 2 diabetes [38–40]. In the light of these reports and our current results, SP-C may be essential for the clearing of brain waste not only by regulating the rheological properties of CSF and ISF within the perivascular channels but also by preventing deposition of misfolded CNS proteins.

Notably, our study suffers from a number of limitations. The major limitation of the study is its retrospective design, resulting in a comparatively small study collective with only morphological—not functional—MRI sequences, which were employed within our diagnostic algorithm. More specifically, inter scanner comparability is very limited and of rather semi-quantitative nature when employing inherently distinct morphologically sequences from different scanners. Therefore, future validation of our results necessitates a study collectively investigated with per se quantitative sequences, for example diffusion-weighted imaging.

Furthermore, white matter changes may also be related to small vessel ischemia to some extent. Currently, an accurate, morphology-based discrimination of causes for white matter hyperintensities, more specifically small vessel disease versus CSF congestion, is not accurately feasible.

Therefore, a prospective study investigating a greater number of patients with diffusion-weighted imaging, including perfusion-sensitive *b* values, should be performed as a more functional technique, better allowing for the quantitative assessment of perfusion and diffusion on a microscopic scale [41].

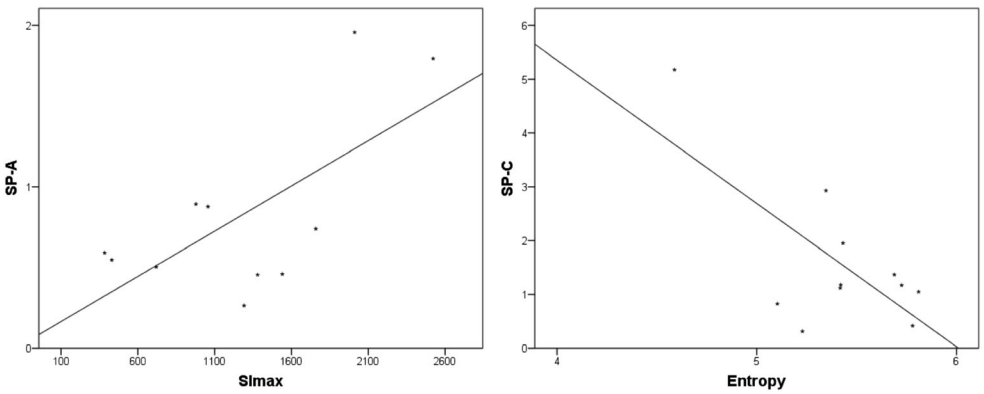

Fig. 3 Summary of the link between measures of deep white matter changes and CSF-SPs A and C in the acute hydrocephalus group, indicating the significance of both SPs for CNS fluid homeostasis and regulation

Conclusions

Both SP-A and SP-C functionally contribute to CSF rheology and brain waste clearance. Thereby, SP-A is predominantly involved in acute stage hydrocephalus and CSF bulk flow, whereas SP-C's main functions are closely associated with microcirculatory CSF flow and ISF exchange with characteristic alterations in chronic hydrocephalic conditions. However, SP-D apparently does not play a major role in this regard.

Acknowledgments The authors acknowledge the (1) support of the Medical Faculty via the Clinician Scientist program and (2) support from the German Research Foundation (DFG) and University Leipzig within the program of Open Access Publishing.

Compliance with Ethical Standards

Conflict of Interest The authors declare that they have no conflict of interest.

References

1. Sunde M, Pham CLL, Kwan AH (2017) Molecular characteristics and biological functions of surface-active and surfactant proteins. Annu Rev Biochem 86:585–608. https://doi.org/10.1146/annurev-biochem-061516-044847
2. Miller R, Fainerman VB, Makievski AV, Krägel J, Grigoriev DO, Kazakov VN, Sinyachenko OV (2000) Dynamics of protein and mixed protein/surfactant adsorption layers at the water/fluid interface. Adv Colloid Interf Sci 86:39–82
3. Fathi-Azarbayjani A, Jouyban A (2015) Surface tension in human pathophysiology and its application as a medical diagnostic tool. Bioimpacts 5:29–44. https://doi.org/10.15171/bi.2015.06
4. Whitsett JA (2014) The molecular era of surfactant biology. Neonatology 105:337–343. https://doi.org/10.1159/000360649
5. Whitsett JA, Wert SE, Weaver TE (2015) Diseases of pulmonary surfactant homeostasis. Annu Rev Pathol 10:371–393. https://doi.org/10.1146/annurev-pathol-012513-104644 Review
6. Whitsett JA, Weaver TE (2015) Alveolar development and disease. Am J Respir Cell Mol Biol 53(1):1–7. https://doi.org/10.1165/rcmb.2015-0128PS
7. Weaver TE, Whitsett JA (1988) Structure and function of pulmonary surfactant proteins. Semin Perinatol 12:213–220
8. Weaver TE (1988) Pulmonary surfactant-associated proteins. Gen Pharmacol 19:361–368
9. Blennow M, Bohlin K (2015) Surfactant and noninvasive ventilation. Neonatology 107:330–336. https://doi.org/10.1159/000381122
10. Enhörning G, Robertson B (1972) Lung expansion in the premature rabbit fetus after tracheal deposition of surfactant. Pediatrics 50:58–66
11. Sardesai S, Biniwale M, Wertheimer F, Garingo A, Ramanathan R (2017) Evolution of surfactant therapy for respiratory distress syndrome: past, present, and future. Pediatr Res 81:240–248. https://doi.org/10.1038/pr.2016.203
12. Schob S, Schicht M, Sel S, Stiller D, Kekulé AS, Paulsen F, Maronde E, Bräuer L (2013) The detection of surfactant proteins A, B, C and D in the human brain and their regulation in cerebral infarction, autoimmune conditions and infections of the CNS. PLoS One 8:e74412. https://doi.org/10.1371/annotation/920eb90c-4f7f-4468-ae9c-1198b7b952fc Erratum in: PLoS One. 2013;8(11). Kekulé, Alexander [corrected to Kekulé, Alexander S]
13. Schob S, Dieckow J, Fehrenbach M, Peukert N, Weiss A, Kluth D, Thome U, Quäschling U et al (2017) Occurrence and colocalization of surfactantproteins A, B, C and D in the developing and adult rat brain. Ann Anat 210:121–127. https://doi.org/10.1016/j.aanat.2016.10.006
14. Krause M, Peukert N, Härtig W, Emmer A, Mahr CV, Richter C, Dieckow J, Puchta J et al (2018) Localization, occurrence, and CSF changes of SP-G, a new surface active protein with assumable immunoregulatory functions in the CNS. Mol Neurobiol 56:2433–2439. https://doi.org/10.1007/s12035-018-1247-x
15. Schob S, Lobsien D, Friedrich B, Bernhard MK, Gebauer C, Dieckow J, Gawlitza M, Pirlich M et al (2016) The cerebral surfactant system and its alteration in hydrocephalic conditions. PLoS One 11:e0160680. https://doi.org/10.1371/journal.pone.0160680
16. Schob S, Weiß A, Surov A, Dieckow J, Richter C, Pirlich M, Horvath-Rizea D, Härtig W et al (2018) Elevated surfactant protein levels and increased flow of cerebrospinal fluid in cranial magnetic resonance imaging. Mol Neurobiol 55:6227–6236. https://doi.org/10.1007/s12035-017-0835-5
17. Schob S, Weiß A, Dieckow J, Richter C, Pirlich M, Voigt P, Surov A, Hoffmann KT et al (2017) Correlations of ventricular enlargement with rheologically active surfactant proteins in cerebrospinal fluid. Front Aging Neurosci 4(8):324. https://doi.org/10.3389/fnagi.2016.00324
18. Litvack ML, Palaniyar N (2010) Review: Soluble innate immune pattern-recognition proteins for clearing dying cells and cellular components: Implications on exacerbating or resolving inflammation. Innate Immun 16:191–200. https://doi.org/10.1177/1753425910369271
19. Palaniyar N (2010) Antibody equivalent molecules of the innate immune system: parallels between innate and adaptive immune proteins. Innate Immun 16:131–137. https://doi.org/10.1177/1753425910370498
20. Boespflug EL, Simon MJ, Leonard E, Grafe M, Woltjer R, Silbert LC, Kaye JA, Iliff JJ (2018) Targeted assessment of enlargement of the perivascular space in Alzheimer's disease and vascular dementia subtypes implicates astroglial involvement specific to Alzheimer's disease. J Alzheimers Dis 66:1587–1597. https://doi.org/10.3233/JAD-180367
21. Iliff JJ, Goldman SA, Nedergaard M (2015) Implications of the discovery of brain lymphatic pathways. Lancet Neurol 14:977–979. https://doi.org/10.1016/S1474-4422(15)00221-5
22. Simon MJ, Iliff JJ (2016) Regulation of cerebrospinal fluid (CSF) flow in neurodegenerative, neurovascular and neuroinflammatory disease. Biochim Biophys Acta 1862:442–451. https://doi.org/10.1016/j.bbadis.2015.10.014
23. Bradley WG, Haughton V, Mardal KA (2016) Cerebrospinal fluid flow in adults. Handb Clin Neurol 135:591–601. https://doi.org/10.1016/B978-0-444-53485-9.00028-3
24. Rasmussen MK, Mestre H, Nedergaard (2018) The glymphatic pathway in neurological disorders. Lancet Neurol 17:1016–1024. https://doi.org/10.1016/S1474-4422(18)30318-1
25. Taoka T, Fujioka M, Matsuo Y, Notoya M, Iwasaki S, Fukusumi A, Nakagawa H, Sakamoto M et al (2004) Signal characteristics of FLAIR related to water content: comparison with conventional spin echo imaging in infarcted rat brain. Magn Reson Imaging 22:221–227
26. Tisell M, Tullberg M, Hellström P, Edsbagge M, Högfeldt M, Wikkelsö C (2011) Shunt surgery in patients with hydrocephalus and white matter changes. J Neurosurg 114:1432–1438. https://doi.org/10.3171/2010.11.JNS10967
27. Kale HA, Muthukrishnan A, Hegde SV, Agarwal V (2017) Intracranial perishunt catheter fluid collections with edema, a sign

of shunt malfunction: correlation of CT/MRI and nuclear medicine findings. AJNR Am J Neuroradiol 38:1754–1757. https://doi.org/10.3174/ajnr.A5291

28. Schob S, Beeskow A, Dieckow J, Meyer HJ, Krause M, Frydrychowicz C, Hirsch FW, Surov A (2018) Diffusion profiling of tumor volumes using a histogram approach can predict proliferation and further microarchitectural features in medulloblastoma. Childs Nerv Syst 34:1651–1656. https://doi.org/10.1007/s00381-018-3846-2
29. Gihr GA, Horvath-Rizea D, Garnov N, Kohlhof-Meinecke P, Ganslandt O, Henkes H, Meyer HJ, Hoffmann KT et al (2018) Diffusion profiling via a histogram approach distinguishes low-grade from high-grade meningiomas, can reflect the respective proliferative potential and progesterone receptor status. Mol Imaging Biol 20:632–640. https://doi.org/10.1007/s11307-018-1166-2
30. Horvath-Rizea D, Surov A, Hoffmann KT, Garnov N, Vörkel C, Kohlhof-Meinecke P, Ganslandt O, Bäzner H et al (2018) The value of whole lesion ADC histogram profiling to differentiate between morphologically indistinguishable ring enhancing lesions-comparison of glioblastomas and brain abscesses. Oncotarget 9:18148–18159. https://doi.org/10.18632/oncotarget.24454
31. Schob S, Münch B, Dieckow J, Quäschling U, Hoffmann KT, Richter C, Garnov N, Frydrychowicz C et al (2018) Whole tumor histogram-profiling of diffusion-weighted magnetic resonance images reflects tumorbiological features of primary central nervous system lymphoma. Transl Oncol 11:504–510. https://doi.org/10.1016/j.tranon.2018.02.006
32. Ringstad G, Vatnehol SAS, Eide PK (2017) Glymphatic MRI in idiopathic normal pressure hydrocephalus. Brain 140(10):2691–2705. https://doi.org/10.1093/brain/awx191
33. Eide PK, Ringstad G (2018) Delayed clearance of cerebrospinal fluid tracer from entorhinal cortex in idiopathic normal pressure hydrocephalus: a glymphatic magnetic resonance imaging study. J Cereb Blood Flow Metab 27:271678X18760974. https://doi.org/10.1177/0271678X18760974
34. Khubchandani KR, Snyder JM (2001) Surfactant protein A (SP-A): the alveolus and beyond. FASEB J 15:59–69
35. Nayak A, Dodagatta-Marri E, Tsolaki AG, Kishore U (2012) An insight into the diverse roles of surfactant proteins, SP-A and SP-D in innate and adaptive immunity. Front Immunol 3:131. https://doi.org/10.3389/fimmu.2012.00131
36. Vieira F, Kung JW, Bhatti F (2017) Structure, genetics and function of the pulmonary associated surfactant proteins A and D: the extra-pulmonary role of these C type lectins. Ann Anat 211:184–201. https://doi.org/10.1016/j.aanat.2017.03.002
37. Verheggen ICM, Van Boxtel MPJ, Verhey FRJ, Jansen JFA, Backes WH (2018) Interaction between blood-brain barrier and glymphatic system in solute clearance. Neurosci Biobehav Rev 90:26–33. https://doi.org/10.1016/j.neubiorev.2018.03.028
38. Willander H, Hermansson E, Johansson J, Presto J (2011) BRICHOS domain associated with lung fibrosis, dementia and cancer–a chaperone that prevents amyloid fibril formation? FEBS J 278:3893–3904. https://doi.org/10.1111/j.1742-4658.2011.08209.x
39. Oskarsson ME, Hermansson E, Wang Y, Welsh N, Presto J, Johansson J, Westermark GT (2018) BRICHOS domain of Bri2 inhibits islet amyloid polypeptide (IAPP) fibril formation and toxicity in human beta cells. Proc Natl Acad Sci U S A 115:E2752–E2761. https://doi.org/10.1073/pnas.1715951115
40. Knight SD, Presto J, Linse S, Johansson J (2013) The BRICHOS domain, amyloid fibril formation, and their relationship. Biochemistry 52:7523–7531. https://doi.org/10.1021/bi400908x
41. Demiral ŞB, Tomasi D, Sarlls J, Lee H, Wiers CE, Zehra A, Srivastava T, Ke K et al (2019) Apparent diffusion coefficient changes in human brain during sleep - does it inform on the existence of a glymphatic system? Neuroimage 185:263–273. https://doi.org/10.1016/j.neuroimage.2018.10.043